The EMBO Journal (2005) 24, 919–928 | © 2005 European Molecular Biology Organization | All Rights Reserved 0261-4189/05
www.embojournal.org

THE EMBO JOURNAL

Mechanisms of photoprotection and nonphotochemical quenching in pea light-harvesting complex at 2.5 Å resolution

Jörg Standfuss[1], Anke C Terwisscha van Scheltinga[1], Matteo Lamborghini and Werner Kühlbrandt*

Max Planck Institute of Biophysics, Department of Structural Biology, Frankfurt am Main, Germany

The plant light-harvesting complex of photosystem II (LHC-II) collects and transmits solar energy for photosynthesis in chloroplast membranes and has essential roles in regulation of photosynthesis and in photoprotection. The 2.5 Å structure of pea LHC-II determined by X-ray crystallography of stacked two-dimensional crystals shows how membranes interact to form chloroplast grana, and reveals the mutual arrangement of 42 chlorophylls *a* and *b*, 12 carotenoids and six lipids in the LHC-II trimer. Spectral assignment of individual chlorophylls indicates the flow of energy in the complex and the mechanism of photoprotection in two close chlorophyll *a*–lutein pairs. We propose a simple mechanism for the xanthophyll-related, slow component of nonphotochemical quenching in LHC-II, by which excess energy is transferred to a zeaxanthin replacing violaxanthin in its binding site, and dissipated as heat. Our structure shows the complex in a quenched state, which may be relevant for the rapid, pH-induced component of nonphotochemical quenching.

The EMBO Journal (2005) **24,** 919–928. doi:10.1038/sj.emboj.7600585; Published online 17 February 2005
Subject Categories: structural biology; plant biology
Keywords: crystal structure; energy transfer; light harvesting; membrane protein; photosynthesis

Introduction

The plant light-harvesting complex of photosystem II (LHC-II) accounts for roughly 30% of the total protein in chloroplast membranes (Peter and Thornber, 1991), which makes it the most abundant membrane protein on Earth. The complex has four distinct but related roles in plant photosynthesis: first and foremost, it collects excitation energy and transfers it to the reaction centres of photosystems (PS) II and I (van Amerongen and Dekker, 2003). Another important role of LHC-II is the distribution of excitation energy between PS II and I, regulated through phosphorylation of LHC-II at its N-terminus (Allen and Forsberg, 2001). Third, LHC-II is largely responsible for the organisation of the plant photosynthetic system by maintaining the tight appression of thylakoid membranes in chloroplast grana (Allen and Forsberg, 2001). Finally, LHC-II prevents damage to the photosynthetic system by several different mechanisms when there is too much light. Potentially harmful chlorophyll (Chl) triplets are quenched by carotenoids in the complex, while a special mechanism, referred to as nonphotochemical quenching (NPQ), has evolved in plants to dissipate excess energy as heat.

The LHC-II family comprises several Chl-protein complexes with similar polypeptide sequences, structure and function (Jansson, 1999). The main LHC-II has three polypeptide components (Lhcb1, b2 and b3) of ~232 amino acids with different tendencies to become phosphorylated and to form trimers (Standfuss and Kühlbrandt, 2004). Each LHC-II polypeptide binds 14 molecules of Chl of two varieties (*a* and *b*), four carotenoids of three different kinds and two different lipids.

The functional unit of LHC-II is the trimer, a compact pigment protein assembly with a local Chl concentration around 300 mM. This is the form in which the complex is isolated from chloroplast membranes by mild detergent treatment. Isolated LHC-II crystallises readily in two (Kühlbrandt *et al*, 1983) and three dimensions (Kühlbrandt, 1987). Electron microscopy (EM) and electron diffraction of two-dimensional (2D) crystals yielded the first atomic model of LHC-II (Kühlbrandt *et al*, 1994), revealing the position of 12 Chls and two carotenoids. The carotenoids were assigned to lutein (Lut), based on their central position in the monomer. The 12 Chls were tentatively assigned to Chl *a* or *b*, depending on their distance to the Luts. These assignments were broadly confirmed by experiments (Remelli *et al*, 1999; Rogl and Kühlbrandt, 1999; Yang *et al*, 1999; Rogl *et al*, 2002).

A full understanding of the trapping, transfer and controlled annihilation of excitation energy by LHC-II requires a structure at higher resolution, for which the 2D membrane crystals were not sufficiently well ordered. Of the two 3D crystal forms of pea LHC-II originally obtained (Kühlbrandt, 1987), the cubic crystals composed of small spherical vesicles (Kühlbrandt, unpublished; Hino *et al*, 2004) did not diffract to high resolution. An *R*32 crystal form similarly composed of icosahedral LHC-II proteoliposomes has recently yielded a 2.72 Å structure of the spinach complex (Liu *et al*, 2004). Another crystal form of LHC-II grows in the shape of hexagonal plates (Kühlbrandt, 1987), consisting of stacks of 2D crystals. These crystals were known to be well ordered, but due to their small size they had to await third-generation synchrotrons for high-resolution data collection. We now report the structure of pea LHC-II at 2.5 Å resolution, determined by X-ray crystallography of thin hexagonal plates.

*Corresponding author. Max Planck Institute of Biophysics, Department of Structural Biology, Max-von-Laue-Strasse 3, 60438 Frankfurt am Main, Germany. Tel.: +49 69 6303 3001; Fax: +49 69 6303 3002; E-mail: werner.kuehlbrandt@mpibp-frankfurt.mpg.de
[1]These authors contributed equally to this work

Received: 25 October 2004; accepted: 26 January 2005; published online: 17 February 2005

Results and discussion

Structure determination

The structure of pea LHC-II was solved by molecular replacement with the 3.4 Å structure determined by EM of 2D crystals (Kühlbrandt *et al*, 1994). It is thus fully independent from the 2.72 Å structure of the spinach complex (Liu *et al*, 2004). Since the C2 crystal form contains three monomers in the asymmetric unit, the trimer was used as a search model. The rotation and translation searches with the atomic EM model gave unambiguous results, in which the highest peaks clearly were the correct solutions (*R*-factor 50.1%, correlation coefficient 0.498). However, as the EM model was incomplete, the resulting phases did not allow immediate fitting of the missing parts. A better approach is to use the EM map itself as a search model, as it contains information from the entire complex including the missing parts. Moreover, since the EM phases are measured directly, they lack model bias. Indeed, this approach gave better statistics (*R*-factor 45.0%, correlation coefficient 0.677) and a more interpretable map (Table I).

Phases were improved and extended by combination with the $P3_121$ data and six-fold averaging. In the resulting map, approximately 85% of the complex could be fitted directly, starting from the 3.4 Å EM structure. Maximum likelihood refinement and maximum entropy completion of the model (Tronrud, 1997; Roversi *et al*, 2000) allowed clear identification of the parts missing in the EM model and accelerated the process of refinement. The free *R*-factor for the final model is 24.1%. This required strong NCS restraints during refinement, due to an almost complete lack of differences between the individual monomers.

All key features that had been identified in the EM model were confirmed at higher resolution. These features include in particular the chain trace in the three membrane-spanning helices and in one short amphipathic helix, the two Luts, the positions of chlorin rings of 12 out of the 14 Chls, nine Chl ligands and the identities of the six central Chls close to the Luts as Chls *a*.

The LHC-II polypeptide

The structure of pea LHC-II is shown in Figure 1. The orientation of the complex in the membrane (Figure 1B) is determined by the N-terminal phosphorylation site on the stromal surface. The LHC-II polypeptide spans the thylakoid membrane three times (Kühlbrandt and Wang, 1991; Kühlbrandt *et al*, 1994), placing the C-terminus on the lumenal side. Previously, the membrane-spanning helices were referred to as A, B and C, and the two short amphiphilic helices on the lumenal side as D and E, in the order in which they were discovered. We propose a new nomenclature in which the helices are referred to by number along the polypeptide chain as helix 1–5 instead of B, E, C, A and D.

Overall, the 0.35 Å root-mean-square deviation of α carbon atoms in pea LHC-II from the spinach complex (Liu *et al*, 2004) indicates a high degree of similarity of the residues present in both structures. However, our structure of the pea

Table I Data collection, molecular replacement and refinement statistics

Data collection and processing		
X-ray source	X11, DESY, Hamburg	ID14-1, ESRF, Grenoble
Wavelength (Å)	0.81	0.934
Resolution range (Å)	50–3.1	50–2.5
Outer shell (Å)	3.2–3.1	2.6–2.5
Space group	$P3_121$	C2
Unit cell (Å, deg)	$a=b=127.5$, $c=180.4$	$a=211.4$, $b=128.0$, $c=62.0$, $\beta=101.8$
No. of measurements	155 599 (10 959)	132 425 (9382)
No. of unique reflections	30 771 (2665)	47 867 (4370)
$I/\sigma(I)$[a]	10.43 (3.62)	8.99 (2.69)
R_{sym}[b]	0.124 (0.381)	0.079 (0.327)
Completeness (%)	97.9 (94.0)	85.6 (70.7)
Molecular replacement		
R-factor[c]	0.452	0.450
Correlation coefficient[d]	0.689	0.667
Refinement		
Resolution range (Å)		50–2.5
Working set		46 853
Test set		990
Non-hydrogen atoms		
Protein		5037
Cofactors		3282
R_{cryst}[c]		0.220
R_{free}[c]		0.241
R.m.s. deviations from ideality		
Bond lengths (Å)		0.011
Bond angles (deg)		1.7

[a]Numbers in parentheses indicate the outer resolution shell.
[b]$R_{sym}=\sum_{hkl}\sum_i|I_i(hkl)-\langle I(hkl)\rangle|/\sum_{hkl}\sum_i I_i(hkl)$, where $I_i(hkl)$ and $\langle I_i(hkl)\rangle$, respectively, are the intensity of the *i*th observation and the mean intensity of reflection *hkl*.
[c]$R=\sum_{hkl}||F_O|-|F_C||/\sum_{hkl}|F_O|$, where F_O and F_C are the observed and calculated structure factor amplitudes, respectively.
[d]Corr. coeff. $=\sum[(|F_O|^2-\langle|F_O|^2\rangle)(|F_C|^2-\langle|F_C|^2\rangle)]/\sqrt{[\sum(|F_O|^2-\langle|F_O|^2\rangle)^2(\sum(|F_C|^2-\langle|F_C|^2\rangle)^2]}$.

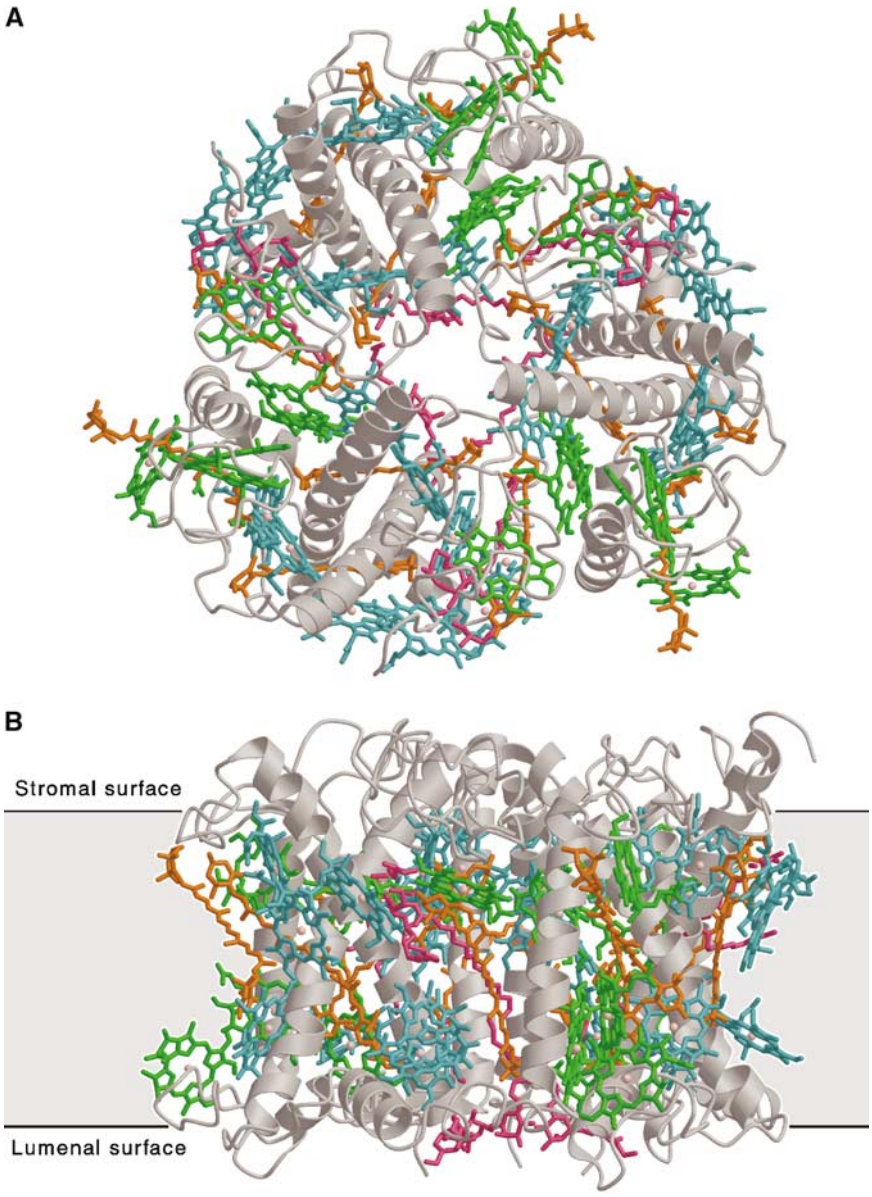

Figure 1 The LHC-II trimer: (**A**) top view from stromal side; (**B**) side view. LHC-II protrudes from a 35 Å lipid bilayer (black lines) by 13 Å on the stromal side and by 8 Å on the lumenal side. Grey, polypeptide; cyan, Chl *a*; green, Chl *b*; orange, carotenoids; pink, lipids.

complex is more complete, as it includes all except the first nine residues, which contain the N-terminal phosphorylation site. These residues are not visible, either due to inherent disorder or because they represent an average of several different Lhcb polypeptides. Native LHC-II consists of at least three different isoforms. The two main gene products, Lhcb1 and Lhcb2, together account for ~90% of the polypeptide. Their sequences are virtually identical (Standfuss and Kühlbrandt, 2004), except at the N-terminus. The simultaneous presence of at least two different sequences might explain why we were unable to trace this part of the polypeptide.

Crystal packing and membrane appression

The 2D crystals making up the 3D lattice of our crystals are in fact crystalline membranes and contain a lipid bilayer (Kühlbrandt *et al*, 1983; Lyon and Unwin, 1988). Adjacent trimers within one layer are related by crystallographic two-fold symmetry in the plane of the membrane and are oriented up and down in this plane. Three pairs of trimers related by a three-fold axis surround a triangular space, most likely filled with disordered lipid and detergent (Figure 2A). Figure 2B shows how the layers stack to form the C2 lattice. The three C-terminal lysines on the lumenal surface of one trimer make different salt bridges to Asp20, Glu31 and Glu150 on the stromal surface of two monomers in the trimer below. While these contacts are not physiological, they are clearly important for the formation of this particular, well-ordered crystal form.

The stromal surface, and in particular the N-terminus, of the LHC-II polypeptide plays an important role in membrane interaction and grana formation. Mild proteolytic treatment of isolated photosynthetic membranes removes the N-terminal segment of LHC-II (Ryrie and Fuad, 1982). Unstacked

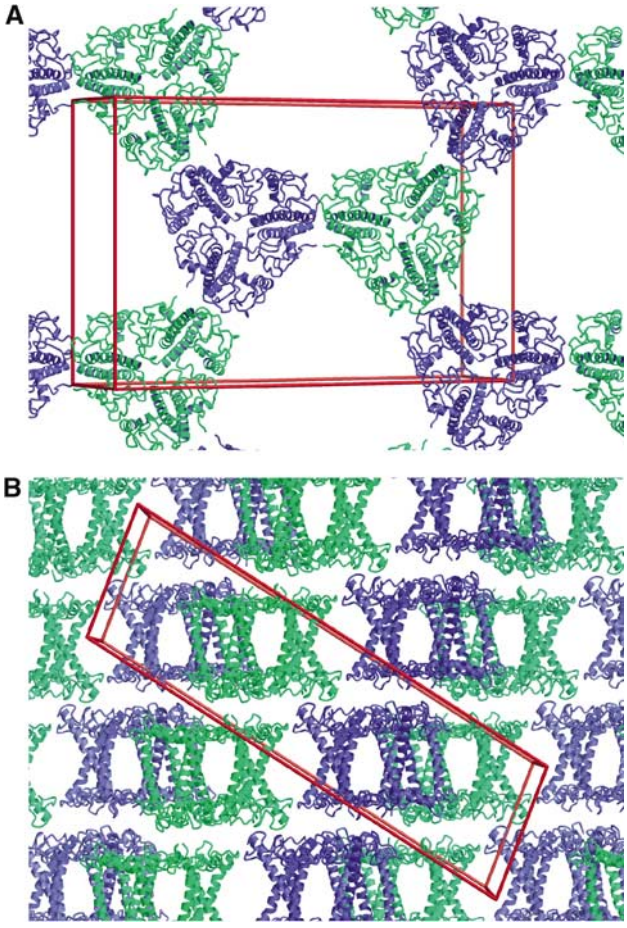

Figure 2 Packing of LHC-II in the C2 crystal lattice: (**A**) top view of a single layer, (**B**) side view of stacked layers. The arrangement of LHC-II trimers within one layer is the same as in 2D crystals (Kühlbrandt *et al*, 1994). The centre of the lipid bilayer contains the crystallographic two-fold axis. Trimers facing up and down are shown in green and blue, respectively. The unit cell ($a = 128.0$ Å; $b = 62.0$ Å; $c = 211.4$ Å; $\alpha = \gamma = 90°$; $\beta = 101.8°$) is shown in red.

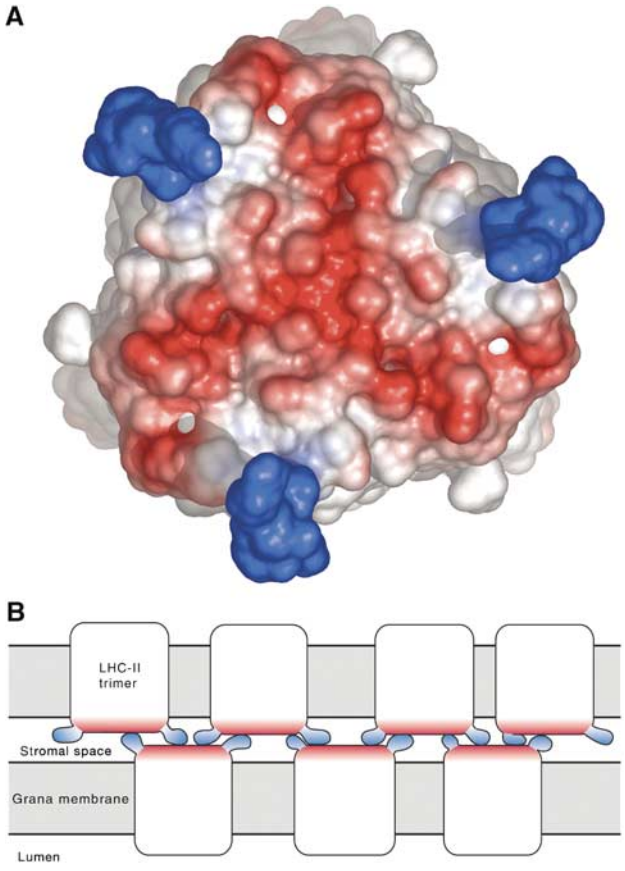

Figure 3 Charge distribution on the stromal surface. Negatively charged areas are red and positively charged areas are blue (**A**). The first nine residues of the polypeptide are disordered and were modelled from the ribosomal protein L39E (PDB code 1JJ2), which has a similar N-terminal sequence. The nonspecific interaction of the positively charged N-terminal peptides of one membrane with the negatively charged surface of trimers in the opposite membrane is likely to play a major role in the cohesion of thylakoid grana, as shown in the schematic diagram (**B**).

grana membranes from which this N-terminal segment has been removed fail to stack under physiological conditions (Steinback *et al*, 1979) but do so at higher ionic strength (Carter and Staehelin, 1980), due to electrostatic charge screening (Barber, 1980). The same behaviour is observed with isolated, purified LHC-II reconstituted into proteoliposomes (McDonnel and Staehelin, 1980; Mullet and Arntzen, 1980; Ryrie *et al*, 1980). Reconstitution of isolated, purified LHC-II into native membranes lacking the complex restores the ability to stack under physiological conditions (Day *et al*, 1984). The contacts between stromal surfaces in our LHC-II crystals provide a lower limit for the closest approach between stromal surfaces in chloroplast grana. Polar and hydrophobic contacts within ~3 Å are observed between Ser12, Gly13, Gly18 and Pro19 with the same region of the monomer opposite in the C2 crystal form. The $P3_121$ crystal form shows different contacts of 3.5–4.5 Å in the same set of stromal surface residues.

The stromal surface of the LHC-II trimer is essentially flat and negatively charged, apart from the first 15 residues, which contain four positive charges (Figure 3). The more complete polypeptide chain in our structure enables us to position this positively charged N-terminal segment in the complex. The first nine residues were modelled on the nearly identical N-terminal sequence of ribosomal protein L39E from *Haloarcula marismortui*. The resulting pattern of positive and negative charges on the stromal membrane surface of LHC-II is striking and immediately suggests a 'velcro'-like, nonspecific interaction of LHC-II trimers in apposed thylakoid membranes, illustrated in the schematic drawing of Figure 3B. This interaction is likely to play a major role in the formation of chloroplast grana, and ensures that the PS II reaction centre is surrounded on all sides by antenna pigments. The remaining net negative charge is overcome by electrostatic screening through mono- and divalent cations. Phosphorylation of the N-terminus by a redox-controlled kinase results in a redistribution of the excitation energy and of LHC-II in the thylakoid membrane. The associated state transitions (reviewed in Allen and Forsberg, 2001) are a key regulatory mechanism in plant photosynthesis.

The two major isoforms in LHC-II are the main factor in membrane appression and grana formation. This is shown by the dramatically increased grana stacks in transgenic tobacco plants, which express pea Lhcb1 constitutively (Labate *et al*,

2004). On the other hand, mutants lacking the Lhcb1 and Lhcb2 gene products nonetheless form grana stacks (Andersson *et al*, 2003). Apparently, other members of the extensive Lhcb family, such as Lhcb4, Lhcb5 and Lhcb6, can replace the main components in this process, as they all have the critical, positively charged N-terminal segment (Pichersky and Jansson, 1996).

Bound lipids

LHC-II binds two different lipids, phosphatidyl glycerol (PG) and digalactosyl diacyl glycerol (DGDG) (Nußberger *et al*, 1993). PG is intimately involved in trimer formation and contains a characteristic 16:1 *trans*-Δ^3-hexadecenoic acid chain (Trémolières, 1991). The structure shows that PG binds at the monomer interface, as anticipated, with one fatty acid chain penetrating deeply into the trimer. The other fatty acid chain has a more peripheral position and extends towards the lipid bilayer. The extended conformation and the potential for π–π interactions with the carotenoid running parallel to it suggest that the fatty acid chain in the deep binding pocket is the *trans*-Δ^3-hexadecenoic chain. This would explain the exquisite specificity of LHC-II for this particular lipid. The polar PG head group coordinates a Chl and a carotenoid and makes polar contacts to Tyr44 and Lys182.

In the pea complex, three DGDG molecules fill a hydrophobic cavity on the three-fold axis on the lumenal side. The DGDG that connects the trimers in crystalline proteoliposomes of spinach LHC-II (Liu *et al*, 2004) is absent, as the corresponding binding site is involved in extensive hydrophobic crystal contacts. The extreme curvature of the proteoliposomes makes it unlikely that the same lipid-trimer configuration can exist in the grana membranes, which are flat on the scale of several 100 μm. Moreover, a DGDG link between LHC-II trimers would result in a planar hexagonal lattice, which has not been observed in native thylakoids.

Spectral assignment of chlorophylls

Like the spinach complex (Liu *et al*, 2004), pea LHC-II contains 14 Chls per monomer. The Chl *a*/*b* ratio of 1.3 indicates eight Chl *a* and six Chl *b*. We introduce a new Chl nomenclature, referring to Chls by numbers 1–14. Chls 1–8 are Chl *a* and Chls 9–14 are Chl *b*. The central Chls 1–6 are the same as Chls *a*1–*a*6 in the original EM structure (Kühlbrandt *et al*, 1994), and Chls 1–3 are related by local near-two-fold symmetry to Chls 4–6 (Figure 4). In the structure of the pea complex, eight Chl *a* and five Chl *b* were identified by difference density maps for the Chl *b* formyl oxygen, and by the presence or absence of hydrogen bonding partners for this group. Chl 9 at the periphery of the trimer had no clear difference density and no potential hydrogen-bonding partner for this group, which is only accessible from the apolar lipid bilayer. The *a*/*b* ratio suggests that this Chl is normally a Chl *b*, in which case the missing H-bonding partner might be supplied by another complex, but the site may equally well be occupied by a Chl *a*.

The orientations of Q_y dipole moments of the 42 Chls in the trimer (Figure 4) sample all directions in space almost evenly to maximise the efficiency of light harvesting. Within experimental error, the positions of Chl head groups are the same as in the spinach complex (Liu *et al*, 2004), except for Chl 2, which is shifted towards Chl 7 by 0.4 Å. The Chl phytyl chains

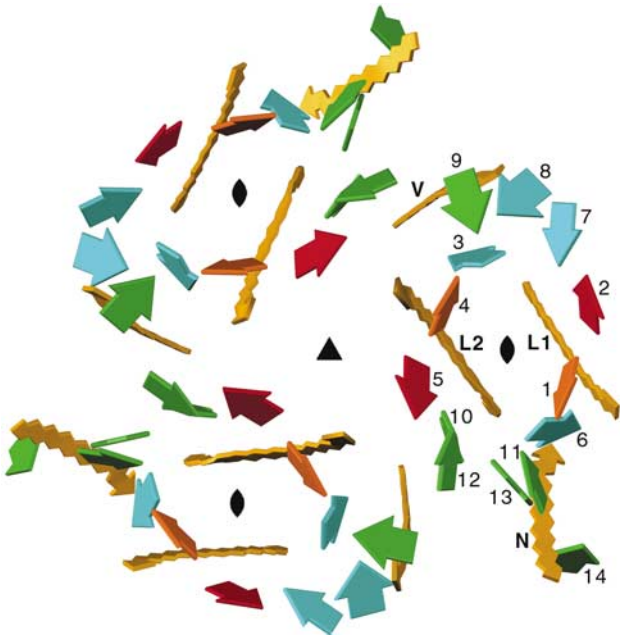

Figure 4 Orientation of Chls and carotenoids in the LHC-II trimer, as seen from the stromal side. The Q_y directions of Chls *a* (1–8) and *b* (9–14) are indicated by short square arrows in the tetrapyrrole ring planes. Carotenoids are yellow arrows in the direction C1–C24. The three-fold axis of the trimer is marked, as are the local two-fold axes that relate one subset of pigments (Chl 1–3 and Lut 1) to another (Chl 4–6 and Lut 2). Red arrows mark symmetry-related low-energy Chl *a* pairs 1, 4 and 2, 5. L, lutein; N, neoxanthin; V, violaxanthin.

were completely fitted, except those of Chls 6, 8, 13 and 14, which extend into the lipid bilayer and are partially disordered.

The 14 Chls in the monomer absorb solar radiation of different wavelengths around 660 ± 20 nm, depending on their chemical environment. The absorption properties of each Chl and hence its position in the LHC-II energy profile are difficult to predict. However, they have been determined experimentally for three Chls *a* (2, 5, 8) and one Chl *b* (12), by low-temperature absorption spectroscopy of LHC-II mutants lacking these pigments (Rogl and Kühlbrandt, 1999; Rogl *et al*, 2002). The spectral positions of the absorption bands of these Chls provide essential guide points for the flow of excitation energy in the LHC-II trimer. Chl 8 is located in a highly apolar environment, consistent with its Q_y band at 659 nm (Rogl and Kühlbrandt, 1999; Rogl *et al*, 2002). This is likely to be the most blue-shifted Chl *a* in LHC-II. Chl 12 has its Q_y band at 650 nm in the middle of the Chl *b* range (Rogl and Kühlbrandt, 1999; Rogl *et al*, 2002).

Chls 2 and 5 form a Chl *a* pair related by a local near-two-fold symmetry (Figure 4) that also extends to the phytyl chains. They are in extensive van der Waals contact with Lut 1 and 2, respectively, through their aligned π systems (Figure 5A). This interaction would cause a red-shift in the absorption of Chls 2 and 5. Chls 1 and 4 form another symmetry-related Chl *a* pair, each of which is coordinated by a Glu that forms an ion bridge with an Arg (Kühlbrandt *et al*, 1994), a polar environment that would cause an electrochromic red-shift. The 4 K absorption spectrum of LHC-II contains a prominent double peak at 671.5 and 676 nm on the red side of the Chl *a* Q_y region (Rogl and

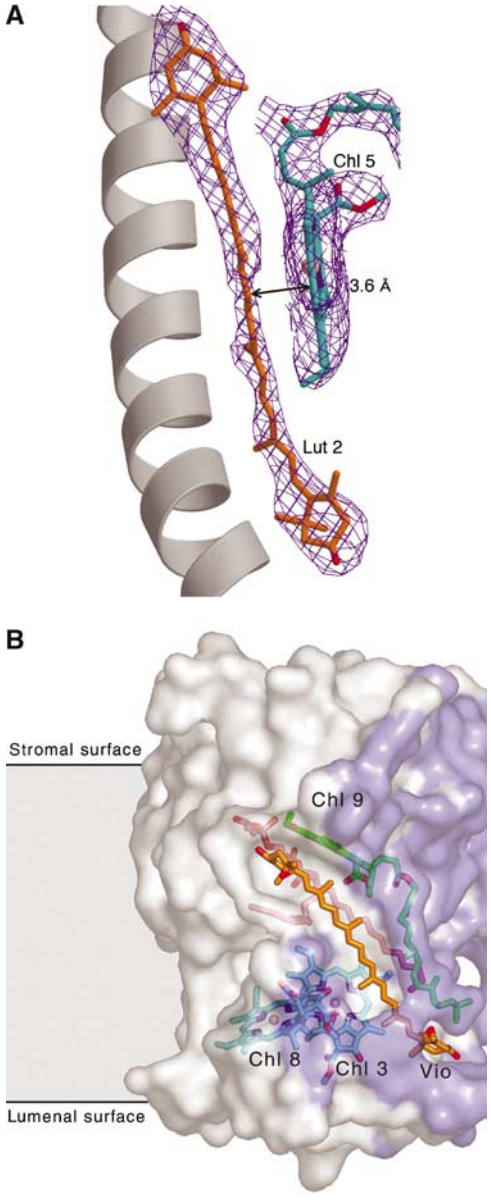

Figure 5 (**A**) Tight Chl *a*–carotenoid interaction in LHC-II. Chl 5 and Lut 2 are in extensive van der Waals contact through their coplanar π systems, causing a red-shift of the Chl *a* absorption. A similar pair of Chl 2 and Lut 1 is related by local two-fold symmetry. The red-shift converts Chls 2 and 5 into sinks for Chl triplets, which are defused by the Luts. (**B**) The Vio binding site. Vio (orange) sits in a pocket on the monomer interface with one end exposed to the lipid bilayer. The 16:1 *trans*-Δ^3-hexadecenoic fatty acid chain of PG (pink) runs along the back of the carotenoid. The phytyl chain of Chl 9 (green) produces a weak repulsive force on one of the epoxide groups. Chls *a* 7 and 8 (cyan; phytyl chains omitted for clarity) are in close proximity. The contact surface between monomers is shown in purple.

Kühlbrandt, 1999; Rogl *et al*, 2002). Clearly, this double peak is due to the two symmetrical, red-shifted Chl *a* pairs.

Carotenoid binding sites

The LHC-II structure of spinach (Liu *et al*, 2004) and pea both show four carotenoids in the same binding sites although there are differences of up to 1 Å in the position and orientation of the head groups. While the orientation of the two Luts in the spinach structure is undetermined, the 2.5 Å map of the pea complex enables us to orient all four carotenoids unambiguously.

The central location of Lut 1 and 2 in the LHC-II monomer was already shown by the EM structure (Kühlbrandt *et al*, 1994). The two additional carotenoids have a more peripheral position. One carotenoid density has an ∼120° bend that suggests a *cis* isomer. Since neoxanthin (Neo) is present in LHC-II with a stoichiometric ratio of one per two Luts, and since all Neo in chloroplast thylakoids is the 9-*cis* isomer (Takaichi and Mimuro, 1998), the assignment of 9-*cis* Neo to this density is unequivocal. Unlike any of the other pigments in LHC-II, the Neo protrudes into the lipid bilayer (Figure 1B). The density is well defined along its entire length, indicating an essentially straight, rigid configuration from C1 to C20. The functional significance of the protruding Neo is not evident. Most likely it interacts with other pigment protein complexes in the membrane, perhaps helping to protect exposed Chls against photodamage.

The fourth carotenoid density in the complex is located at the monomer interface. The rotation of the head groups relative to the planar π system identifies this carotenoid as violaxanthin (Vio). The isolated complex we used for crystallisation contains Lut, Neo and Vio in a ratio of roughly 2:1:0.5. Of all the carotenoids in LHC-II, Vio has the lowest binding affinity (Ruban *et al*, 1999; Hobe *et al*, 2000) and is easily lost during purification, which explains its presence in substoichiometric amounts. However, the occupancy of Vio in our structure is similar to that of the other carotenoids, indicating that trimers with a full complement of carotenoids crystallise selectively. The full occupancy of all four binding sites moreover indicates that they are specific for their respective carotenoid under normal conditions. Recombinant complexes obtained by refolding in the presence of only one carotenoid are therefore of limited value for functional studies.

The Vio binding site is shown in Figure 5B. The OH group at the C1 end of the carotenoid makes a hydrogen bond to the phytyl carbonyl of Chl 10. At the other end, there is a polar contact to a glycerol OH of the PG lipid. Otherwise, the binding pocket is entirely hydrophobic. For most of its length, the carotenoid runs parallel to the *trans*-Δ^3-hexadecenoic acid chain at the monomer interface.

Light harvesting by carotenoids

The carotenoids in LHC-II have a dual function as light-harvesting pigments and in photoprotection. The LHC-II absorption spectrum is clearly dominated by Chls, indicating that the carotenoid contribution to light harvesting in plants is comparatively minor. Carotenoids can transfer energy to Chls either from the excited S_2 state or from the energetically lower S_1 state (Polívka and Sundström, 2004). The S_2 state transmits to the Chl Q_x state (Polívka and Sundström, 2004). This is more efficient than transfer from the S_1 state, but must occur within ∼100 fs to avoid energy loss due to internal S_2–S_1 conversion. This ultrafast energy transfer requires spectral overlap as well as close coplanar contact and vectorial alignment of the carotenoid π system with the Chl Q_x direction, as observed for the Chl 2/Lut 1 and Chl 5/Lut 2 pairs (Figure 5A). We conclude that these two Chl *a* molecules receive energy from the Luts mainly via the S_2–Q_x mechanism. None of the other carotenoids are coplanar with their nearest-neighbour Chls but all are closer than

~6 Å to at least one Chl (Table II). Presumably, they transfer energy to the Chls from the S_1 state, which has a longer lifetime and is less dependent on orientation than distance. Strikingly, the π systems of several Chls are perpendicular to those of the closest carotenoid. This arrangement, observed for Chl 3 and Lut 1, Chl 6 and Lut 2, Chl 6 and Neo, Chl 8 and Vio and Chl 14 and Vio, allows excitation energy transfer but not electron transfer (Dreuw *et al*, 2003) between these pairs of pigments.

Photoprotection

A crucial role of carotenoids in LHC-II is to avert damage from the photosynthetic system. The ability of carotenoids to quench Chl triplet states and thus to prevent the formation of highly reactive singlet oxygen makes them indispensable in the antenna system of green plants. Triplet quenching proceeds by intersystem crossing, either by electron exchange as discussed previously (Kühlbrandt *et al*, 1994) or by the charge-transfer mechanism, which has been shown to be more efficient for singlet transfer (Dreuw *et al*, 2003). Electron exchange merely requires partial orbital overlap and hence close van der Waals contact, while singlet charge-transfer additionally requires coplanar π systems (Dreuw *et al*, 2003).

The overlap of π orbitals would be most pronounced for Lut 1 with Chls 1 and 2, and for Lut 2 with Chls 4 and 5. In addition, the π systems of Lut 1 and 2 are exactly coplanar to those of Chls 2 and 5, with interplane distances of 3.5 and 3.6 Å, respectively (Figure 5A and Table II). Due to their low-lying energy levels (Rogl and Kühlbrandt, 1999; Rogl *et al*, 2002), Chls 2 and 5 act as sinks for any Chl triplets arising in LHC-II. These would then be rapidly defused by the coplanar Luts, presumably through the charge-transfer mechanism.

Proposed mechanism of nonphotochemical quenching in LHC-II

Photosynthesis in green plants depends on a protective mechanism that adapts within minutes or seconds to changing light conditions, for example, when a shade leaf becomes exposed to full sunlight. The excess energy needs to be dissipated in the antenna, to minimise irreversible damage to the photosynthetic system. This process, known as NPQ (Demmig-Adams, 1990), has two components (Niyogi *et al*, 1998). A comparatively slow component is activated within minutes and directly related to the conversion of Vio to zeaxanthin (Zea) in the xanthophyll cycle (Gilmore and Yamamoto, 1992; Horton and Ruban, 1992; Pfundel and Bilger, 1994). A second component of NPQ is induced within seconds by a drop in pH. This fast component seems to be independent of the xanthophyll cycle (Niyogi *et al*, 1998). It may be related to the PsbS protein, a member of the Lhc family, which was found to be absent in *Arabidopsis* mutants deficient in NPQ (Li *et al*, 2000), although its exact role remains enigmatic. The 2.5 Å structure of the pea complex now enables us to propose a mechanism for the slow, xanthophyll-dependent NPQ in LHC-II (Figure 6).

Excitation energy in LHC-II passes to the pigment with the lowest energy level in less than 1 ps. Normally the acceptor is a red-shifted Chl *a*, which would then transmit the energy to neighbouring antenna complexes, and ultimately to the special Chl pair in a reaction centre. Due to its extended π system of 11 conjugated double bonds, Zea has an excited S_1 state considerably below the red-most Chl *a* S_1 state (Frank *et al*, 1994). Zea has the same molecular structure as Vio, except that it lacks the epoxy groups at either end. It is therefore expected to bind more strongly to the hydrophobic Vio site, because it is less polar. The phytyl chain of Chl 9 is in close van der Waals contact (2.8 Å) to one of the epoxy groups (Figure 5B) and therefore would exert a weak repulsive force on Vio, but not on Zea. Indeed, Zea has been shown to bind to LHC-II more strongly than Vio (Ruban *et al*, 1999). Zea can accept energy from Chl Q_y states in all possible orientations, whereas Vio can do so only at very close distances by charge transfer, which requires coplanar π systems (Dreuw *et al*, 2003). None of the Chls close to Vio meet this condition, so that singlet energy transfer from Chl to this pigment is excluded. However, Zea bound to the Vio site would receive all the excitation energy collected in the trimer, via Chl 8 or 9 (Table II). The energy cannot escape back to Chl and is dissipated as heat.

Table II Closest contacts between chlorophylls and carotenoids

Chl in (Kühlbrandt *et al*, 1994)	Chl in (Liu *et al*, 2004)	New nomenclature	Closest carotenoids	Closest π–π contact (Å) (internuclear distance)	Mg^{2+} ligand	H bond to Chl *b* formyl group
Chlorophylls *a*						
*a*1	610	Chl 1	Lut 1	3.3	Glu180 Oε2	
*a*2	612	Chl 2	Lut 1	3.5	Asn183 Oδ1	
*a*3	613	Chl 3	Lut 1	5.0	Gln197 Oε1	
*a*4	602	Chl 4	Lut 2	3.2	Glu65 Oε2	
*a*5	603	Chl 5	Lut 2	3.6	His68 Nε2	
*a*6	604	Chl 6	Lut 2	4.8	Wat-Gly78 O	
*b*2	611	Chl 7	Lut 1	9.1	PG O4	
*b*3	614	Chl 8	Lut 1	8.0	His212 Nε2	
Chlorophylls *b*						
—	601	Chl 9	Lut 2	8.0	Tyr24 O	—
*a*7	607	Chl 10	Lut 2	5.1	Wat-Chl 13 OMC	Gln131 Nε1
*b*1	608	Chl 11	Neo	4.3	Wat-Val138 O	Leu148 N
*b*5	609	Chl 12	Lut 2	7.8	Glu139 Oε2	Gln131 Nε1
*b*6	606	Chl 13	Lut 2	4.9	Wat-Gln131 Oε2	Wat-Chl 10 Mg
—	605	Chl 14	Neo	12.3	Val119 O	Ser123 N

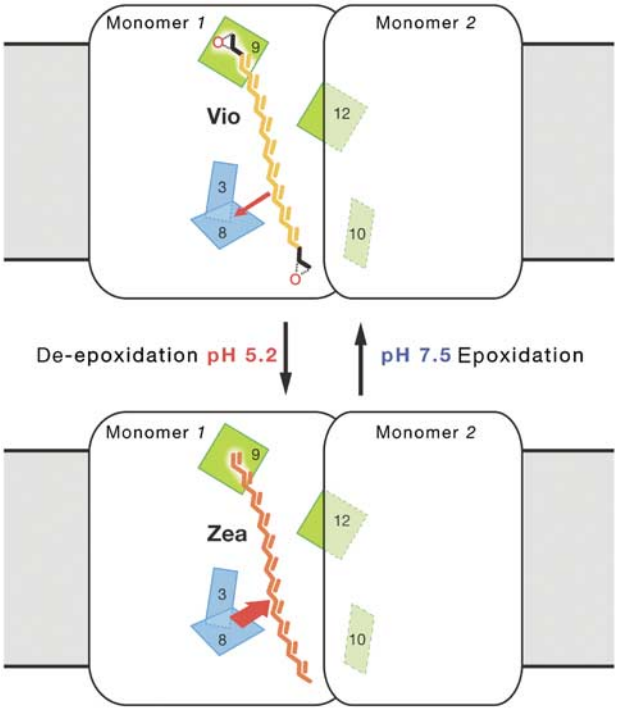

Figure 6 NPQ in LHC-II. Plants depend on an efficient system for rapid defusion of excess light energy. The structure of pea LHC-II suggests a simple mechanism for this process. Due to its short π system of nine conjugated double bonds, Vio donates excitation energy to nearby Chls (thin red arrow). Zea has a more extended π system of 11 double bonds and therefore is able to accept energy from any Chl. When a Zea binds to the Vio site, the energy collected in the LHC-II trimer is transferred to this carotenoid, most likely via the nearby Chl 8 (thick red arrow). The energy cannot escape and is dissipated as heat. This process is easily regulated by the pH-activated, lumenal Vio de-epoxidase, which converts Vio to Zea as the photosynthetic activity of the chloroplast causes the lumenal pH to drop.

Our structure suggests a simple and elegant mechanism (Figure 6) for regulating the slow, xanthophyll-dependent component of NPQ through the activity of the Vio de-epoxidase, a pH-activated lumenal enzyme (Hager, 1969; Demmig-Adams, 1990; Pfundel and Bilger, 1994; Hieber *et al*, 2000). As the photosynthetic rate increases, the pH of the lumen drops and the de-epoxidase is turned on. Due to its low binding affinity, Vio equilibrates with a pool of the free carotenoid in the membrane, where it is converted to Zea via antheraxanthin by the de-epoxidase. We propose that Zea binds to the Vio site, converting an LHC-II trimer into an energy sink. As more and more LHC-II trimers bind Zea, less energy is transferred to the reaction centres, the photosynthetic rate decreases, the pH in the lumen rises and the de-epoxidase is inactivated. Zea is converted back to Vio by the stromal Zea epoxidase (Demmig-Adams, 1990; Hieber *et al*, 2000), and rebinds to its site in LHC-II. This cycle repeats as soon as the absorbed light energy exceeds the amount that can be used for photosynthesis.

There is strong and increasing evidence for this proposed role of LHC-II in NPQ. It was found that addition of Zea to isolated LHC-II rapidly induces fluorescence quenching (Wentworth *et al*, 2001), exactly as our model predicts. Vio bound to *in vitro* refolded LHC-II is de-epoxidised to Zea by the de-epoxidase (Jahns *et al*, 2001), again as predicted by our model. Mutants lacking Lhcb1 and Lhcb2 have a 30% reduced capacity for NPQ (Andersson *et al*, 2003). Probably, the actual contribution to NPQ by the main LHC-II components is considerably higher than this figure suggests, because the absence of Lhcb1 and Lhcb2 is partially compensated by Lhcb5, which is expressed at higher levels in these mutants and also participates in NPQ (Ruban and Horton, 1995). Finally, transgenic tobacco plants expressing Lhcb1 from pea show a large increase in the level of NPQ (Labate *et al*, 2004).

An attractive feature of our proposed mechanism is that it does not require a conformational change in the antenna. An NPQ mechanism based on a pH-induced conformational change within LHC-II has often been postulated (Ruban *et al*, 1999), most recently by Liu *et al* (2004). This change is supposed to happen at pH 5.5 by bringing two Chls into close proximity, so that they form a quenching pair. Under high light conditions where NPQ occurs, the pH in the thylakoid lumen drops to 5.2–6.0 (Demmig-Adams, 1990). The lower limit is set by the pH optimum of the Vio de-epoxidase at 5.2 (Hager, 1969), which, according to more recent measurements is actually 5.6 *in vivo* (Günther *et al*, 1994). The crystals we used for structure determination grow at pH 5.5, close to the lowest pH experienced by LHC-II in an intact leaf cell. By contrast, the crystals that yielded the structure of the spinach complex (Liu *et al*, 2004) were grown at pH 7.5, yet we do not observe a pH-induced conformational change in the protein structure. Thus, there is no experimental evidence for such a change, and our proposed mechanism of Zea-dependent NPQ in LHC-II suggests that there is no need for it.

A quenched state of LHC-II

The *in vitro* aggregates of LHC-II, obtained by salt precipitation of the detergent-solubilised complex over a wide pH range, are microcrystalline stacks (McDonnel and Staehelin, 1980; Mullet and Arntzen, 1980; Ryrie *et al*, 1980) of 2D crystals (Kühlbrandt *et al*, 1983), exactly as in our hexagonal plate crystals. The lateral contacts between trimers within one layer in these crystals are entirely hydrophobic, involving the interaction of side chains of Leu164 and Leu166 on the stromal side of one complex with Leu85, Val90 and Leu113 on the lumenal side of another, and the phytyl chains of Chls 1, 2 and 7. This large hydrophobic contact surface must provide the main driving force for the formation of these aggregates and 2D crystals of LHC-II.

It is well known that the Chl fluorescence of LHC-II aggregates is quenched (Mullet and Arntzen, 1980; Ide *et al*, 1987; Gillbro *et al*, 1988; Mullineaux *et al*, 1993). We therefore have good reasons to believe that our structure shows a quenched state of the complex. This might simply be caused by Chls brought into close contact in the crystalline state. However, inspection of the pigments near the trimer interface in the 2D lattice indicated that closest intertrimer distance between Chls is 17.6 Å (Mg–Mg of Chls2), considerably longer than the shortest Chl–Chl distances within one trimer. The fluorescence quenching must therefore have another reason, manifest in a difference in the pigment arrangement compared to the unquenched state. Presumably, this is present in the structure of Liu *et al* (2004), as the LHC-II trimers in the proteoliposomes are not in direct contact but separated by lipid molecules. The only difference we were able to detect that could potentially account for the quenching effect is the

0.4 Å displacement of Chl 2 towards Chl 7. Such a small shift may be sufficient for fluorescence quenching, because energy transfer depends on the sixth power of distance (Förster, 1949). We are currently investigating this possibility. Chl 2 is close to the large contact surface that gives rise to the crystalline aggregates, and its displacement is evidently a result of the strong hydrophobic interaction between adjacent trimers. It is worth noting that the same interaction between LHC-II trimers cannot occur *in vivo*, because of the inherent, in-plane two-fold symmetry of the 2D lattice, whereas in the thylakoid membrane, all trimers face the same way. The quenched state of LHC-II we observe may thus be simply the result of an accidental complementarity of hydrophobic contact surfaces in the LHC-II crystals, and as such unrelated to NPQ. On the other hand, if a similar hydrophobic contact with a different thylakoid membrane protein, perhaps upon a pH-induced interaction with LHC-II, were to exert the same force on Chl 2, this quenched state may be relevant for the rapid, xanthophyll-independent component of NPQ.

Materials and methods

Isolation and purification

Pea plants (*Pisum sativum*) were grown on vermiculite for 15–18 days in a period of 10 h light (~10 000–15 000 lux) and 14 h dark in a growth room at 20°C and 45% humidity. Thylakoid membranes were isolated from pea leaves as described (Burke *et al*, 1978; Kühlbrandt *et al*, 1983). The purified protein was dissolved in 1% w/v *n*-nonyl-β-D-glucoside at a Chl concentration of 3.5 mg/ml. Before crystallization, the sample was further concentrated by centrifugation for 4 h at 100 000 r.p.m. The light green supernatant was removed and the remaining solution adjusted to a final Chl concentration of 4.5 mg/ml and an *n*-nonyl-β-D-glucoside concentration of 1.6% w/v.

Crystallisation

LHC-II crystals were grown by hanging-drop vapour diffusion at 20°C, by mixing 1 µl of protein solution with an equal volume of reservoir solution (10–15% polyethylene glycol 350 monomethyl ether, 50 mM morpholinoethanesulphonic acid buffer pH 5.2–5.6, 10–15% glycerol, 20 mM NaCl). Thin hexagonal plates appear within 3–5 weeks and grow to a size of $400 \times 400 \times 20\,\mu m^3$. They belong to space groups $P3_121$ or C2 and diffract beyond 2.2 Å.

Data collection

Crystals were flash frozen in liquid ethane or a cryo steam (100 K, Oxford Cryosystems). Diffraction data were collected at 100 K on beamline ID14-1 at the European Synchrotron Radiation Facility or at the EMBL beamline X11 at the Deutsches Elektronen Synchrotron. Data were indexed and scaled with XDS (Kabsch, 1988, 1993).

Structure determination and refinement

The structure was solved by molecular replacement with the 3.4 Å map of pea LHC-II determined by electron crystallography (Kühlbrandt *et al*, 1994). A trimer was cut from the map using the USF program suite (Kleywegt and Jones, 1999). The resulting map was used as a search model for molecular replacement with MOLREP (Vagin and Teplyakov, 1997) for both the C2 and $P3_121$ data. Initial phases were improved and extended with the program DMMULTI (Cowtan, 1994) by combining multicrystal averaging over the three monomers in the C2 crystal and three in the $P3_121$ crystal with solvent flattening and histogram mapping. The atomic EM model, which contained about 75% of all atoms in the complex, was placed into the 2.5 Å C2 electron density map with the pea Lhcb1 polypeptide sequence and improved by alternating cycles of manual rebuilding with O (Jones *et al*, 1991) and refinement using the BUSTER-TNT suite (Tronrud, 1997; Roversi *et al*, 2000). Figures were prepared with BOBSCRIPT (Esnouf, 1997) and PYMOL (WL DeLano, The PyMOL Molecular Graphics System (2002), http://www.pymol.org).

Rebuilding and refinement started from the EM model and converged to a free *R*-factor of 24.1 (Table I). Strong NCS restraints were maintained throughout refinement. The polypeptide geometry is excellent (Table I). The Ramachandran plot shows only one outlier, Val119, which coordinates a Chl by its main-chain carbonyl.

Final coordinates and structure factors have been deposited in the Protein Data Bank (ID codes 2bhw and r2bhwsf, respectively).

Acknowledgements

We thank Heidi Betz for excellent technical assistance, Gitte Mohsin and Paolo Lastrico for help with the figures, Wolfgang Kabsch for help with XDS and Andreas Dreuw for discussions on energy transfer. We acknowledge the European Synchrotron Radiation Facility, Grenoble, the EMBL at Deutsches Elektronen Synchrotron, Hamburg, and the Swiss Light Source, Paul Scherrer Institut, Villigen, Switzerland for provision of synchrotron radiation facilities, and thank their beamline staff for assistance during data collection.

References

Allen JF, Forsberg J (2001) Molecular recognition in thylakoid structure and function. *Trends Plant Sci* **6:** 317–326

Andersson J, Wentworth M, Walters RG, Howard CA, Ruban AV, Horton P, Jansson S (2003) Absence of the Lhcb1 and Lhcb2 proteins of the light-harvesting complex of photosystem II—effects on photosynthesis, grana stacking and fitness. *Plant J* **35:** 350–361

Barber J (1980) Membrane surface charges and potentials in relation to photosynthesis. *Biochim Biophys Acta* **594:** 253–308

Burke JJ, Ditto CL, Arntzen CJ (1978) Involvement of the light-harvesting complex in cation regulation of excitation energy distribution in chloroplasts. *Arch Biochem Biophys* **187:** 252–263

Carter DP, Staehelin LA (1980) Proteolysis of chloroplast thylakoid membranes. II. Evidence for the involvement of the light-harvesting chlorophyll *a*/*b*-protein complex in thylakoid stacking and for effects of magnesium ions on photosystem II-light-harvesting complex aggregates in the absence of membrane stacking. *Arch Biochem Biophys* **200:** 374–386

Cowtan K (1994) *Joint CCP4 ESF-EACBM. Newsl Protein Crystallogr* **31:** 34–38

Day DA, Ryrie IJ, Fuad N (1984) Investigations of the role of the main light-harvesting chlorophyll-protein complex in thylakoid membranes. Reconstitution of depleted membranes from intermittent-light-grown plants with the isolated complex. *J Cell Biol* **97:** 163–172

Demmig-Adams B (1990) Carotenoids and photoprotection in plants: a role for the xanthophyll zeaxanthin. *Biochim Biophys Acta* **1020:** 1–24

Dreuw A, Fleming GR, Head-Gordon M (2003) Chlorophyll fluorescence quenching by xanthophylls. *Phys Chem Chem Phys* **5:** 3247–3256

Esnouf RM (1997) An extensively modified version of MolScript that includes greatly enhanced coloring capabilities. *J Mol Graph* **15:** 132–134

Förster VT (1949) Experimentelle und theoretische Untersuchung des zwischenmolekularen Uebergangs von Elektronenanregungsenergie. *Zeitschrift für Naturforschung* **4:** 321–327

Frank HA, Cua A, Chynwat V, Young A, Gosztola D, Wasielewski MR (1994) Photophysics of the carotenoids associated with the xanthophyll cycle in photosynthesis. *Photosynth Res* **41:** 389–395

Gillbro T, Sandström A, Spangfort M, Sundström V, van Grondelle R (1988) Excitation energy annihilation in aggregates of chlorophyll *a/b* complexes. *Biochem Biophy Acta* **934:** 369–374

Gilmore AM, Yamamoto HY (1992) Dark induction of zeaxanthin-dependent nonphotochemical fluorescence quenching mediated by ATP. *Proc Natl Acad Sci USA* **89:** 1899–1903

Günther G, Thiele A, Laasch H (1994) A new method for the determination of the transthylakoid pH gradient in isolated chloroplasts: the pH-dependent activity of violaxanthin de-epoxidase. *Plant Sci* **102:** 19–30

Hager A (1969) Light dependent decrease of pH-value in a chloroplast compartment causing enzymatic interconversion of violaxanthin to zeaxanthin—relations to photophosphorylation. *Planta* **89:** 224–243

Hieber AD, Bugos RC, Yamamoto HY (2000) Plant lipocalins: violaxanthin de-epoxidase and zeaxanthin epoxidase. *Biochim Biophys Acta* **1482:** 84–91

Hino T, Kanamori E, Shen JR, Kouyama T (2004) An icosahedral assembly of the light-harvesting chlorophyll *a/b* protein complex from pea chloroplast thylakoid membranes. *Acta Crystallogr D* **60:** 803–809

Hobe S, Niemeier H, Bender A, Paulsen H (2000) Carotenoid binding sites in LHCIIb. Relative affinities towards major xanthophylls of higher plants. *Eur J Biochem* **267:** 616–624

Horton P, Ruban AV (1992) Regulation of photosystem II. *Photosynth Res* **34:** 375–385

Ide JP, Klug DR, Kühlbrandt W, Giorgi LB, Porter G (1987) The state of detergent solubilised light-harvesting chlorophyll-*a/b* protein complex as monitored by picosecond time-resolved fluorescence and circular dichroism. *Biochem Biophy Acta* **893:** 349–364

Jahns P, Wehner A, Paulsen H, Hobe S (2001) De-epoxidation of violaxanthin after reconstitution into different carotenoid binding sites of light-harvesting complex II. *J Biol Chem* **276:** 22154–22159

Jansson S (1999) A guide to the Lhc genes and their relatives in *Arabidopsis*. *Trends Plant Sci* **4:** 236–240

Jones TA, Zou J-Y, Cowan SW, Kjeldgaard M (1991) Improved methods for building protein models in electron-density maps and the location of errors in these models. *Acta Crystallogr A* **47:** 110–119

Kabsch W (1988) Automatic indexing of rotation diffraction patterns. *J Appl Crystallogr* **21:** 67–71

Kabsch W (1993) Automatic processing of rotation diffraction data from crystals of initially unknown symmetry and cell constants. *J Appl Crystallogr* **26:** 795–800

Kleywegt GJ, Jones TA (1999) Software for handling macromolecular envelopes. *Acta Crystallor D* **55:** 941–944

Kühlbrandt W (1987) Three-dimensional crystals of the light-harvesting chlorophyll *a/b* protein complex from pea chloroplasts. *J Mol Biol* **194:** 757–762

Kühlbrandt W, Thaler T, Wehrli E (1983) The structure of membrane crystals of the light-harvesting chlorophyll *a/b* protein complex. *J Cell Biol* **96:** 1414–1424

Kühlbrandt W, Wang DN (1991) Three-dimensional structure of plant light-harvesting complex determined by electron crystallography. *Nature* **350:** 130–134

Kühlbrandt W, Wang DN, Fujiyoshi Y (1994) Atomic model of plant light-harvesting complex by electron crystallography. *Nature* **367:** 614–621

Labate MTV, Ko K, Ko ZW, Costa Pinto LSR, Real MJUD, Romano MR, Barja PR, Granell A, Friso G, van Wijk KJ, Brugnoli E, Labate CA (2004) Constitutive expression of pea *Lhcb1-2* in tobacco affects plant development, morphology and photosynthetic capacity. *Plant Mol Biol* **55:** 701–714

Li X-P, Björkman O, Shih C, Grossman AR, Rosenquist M, Jansson S, Niyogi KK (2000) A pigment-binding protein essential for regulation of photosynthetic light harvesting. *Nature* **403:** 391–395

Liu Z, Yan H, Wang K, Kuang T, Zhang J, Gui L, An X, Chang W (2004) Crystal structure of spinach major light-harvesting complex at 2.72 Å resolution. *Nature* **428:** 287–292

Lyon MK, Unwin PNT (1988) Two-dimensional structure of the light-harvesting chlorophyll *a/b* complex by cryoelectron microscopy. *J Cell Biol* **106:** 1515–1523

McDonnel A, Staehelin LA (1980) Adhesion between liposomes mediated by the chlorophyll *a/b* light-harvesting complex isolated from chloroplast membranes. *J Cell Biol* **84:** 40–56

Mullet JE, Arntzen CJ (1980) Simulation of grana stacking in a model membrane system. Mediation by a purified light-harvesting pigment-protein complex from chloroplasts. *Biochim Biophys Acta* **589:** 100–117

Mullineaux CW, Pascal AA, Horton P, Holzwarth AR (1993) Excitation-energy quenching in aggregates of the LHC II chlorophyll-protein complex: a time-resolved fluorescence study. *Biochem Biophy Acta* **1141:** 23–28

Niyogi KK, Grossman AR, Björkman O (1998) Arabidopsis mutants define a central role for the xanthophyll cycle in the regulation of photosynthetic energy conversion. *Plant Cell* **10:** 1121–1134

Nußberger S, Dörr K, Wang DN, Kühlbrandt W (1993) Lipid–protein interactions in crystals of plant light-harvesting complex. *J Mol Biol* **234:** 347–356

Peter GF, Thornber JP (1991) Biochemical composition and organization of higher plant photosystem II light-harvesting pigment-proteins. *J Biol Chem* **266:** 16745–16754

Pfundel E, Bilger W (1994) Regulation and possible function of the violaxanthin cycle. *Photosynth Res* **42:** 89–109

Pichersky E, Jansson S (1996) The light-harvesting chlorophyll *a/b* binding polypeptides and their genes in angiosperm and gymnosperm species. In *Oxygenic Photosynthesis: The Light Reactions*, Ort DR, Yocum CF (eds) Vol. 28, pp 507–521

Polívka T, Sundström V (2004) Ultrafast dynamics of carotenoid excited states—from solution to natural and artificial systems. *Chem Rev* **104:** 2021–2071

Remelli R, Varotto C, Sandona D, Croce R, Bassi R (1999) Chlorophyll binding to monomeric light-harvesting complex. A mutation analysis of chromophore-binding residues. *J Biol Chem* **274:** 33510–33521

Rogl H, Kühlbrandt W (1999) Mutant trimers of light-harvesting complex II exhibit altered pigment content and spectroscopic features. *Biochemistry* **38:** 16214–16222

Rogl H, Schödel R, Lokstein H, Kühlbrandt W, Schubert A (2002) Assignment of spectral substructures to pigment-binding sites in higher plant light-harvesting complex LHC-II. *Biochemistry* **41:** 2281–2287

Roversi P, Blanc E, Vonrhein C, Evans G, Bricogne G (2000) Modelling prior distributions of atoms for macromolecular refinement and completion. *Acta Crystallogr D* **56:** 1316–1323

Ruban AV, Horton P (1995) Regulation of nonphotochemical quenching of chlorophyll fluorescence in plants. *Aust J Plant Physiol* **22:** 221–230

Ruban AV, Lee PJ, Wentworth M, Young AJ, Horton P (1999) Determination of the stoichiometry and strength of binding of xanthophylls to the photosystem II light harvesting complexes. *J Biol Chem* **274:** 10458–10465

Ryrie IJ, Anderson JM, Goodchild DJ (1980) The role of the light-harvesting chlorophyll *a/b* protein complex in chloroplast membrane stacking. Cation-induced aggregation of reconstituted proteoliposomes. *Eur J Biochem* **107:** 345–354

Ryrie IJ, Fuad N (1982) Membrane adhesion in reconstituted proteoliposomes containing the light-harvesting chlorophyll *a/b*-protein complex: the role of charged surface groups. *Arch Biochem Biophys* **214:** 475–488

Standfuss J, Kühlbrandt W (2004) The three isoforms of the light-harvesting complex II: spectroscopic features, trimer formation, and functional roles. *J Biol Chem* **279:** 36884–36891

Steinback KE, Burke JJ, Arntzen CJ (1979) Evidence for the role of surface-exposed segments of the light-harvesting complex in cation-mediated control of chloroplast structure and function. *Arch Biochem Biophys* **195:** 546–557

Takaichi S, Mimuro M (1998) Distribution and geometric isomerism of neoxanthin in oxygenic phototrophs: 9′-*cis*, a sole molecular form. *Plant Cell Physiol* **39:** 968–977

Trémolières A (1991) Lipid–protein interactions in relation to light energy distribution in photosynthetic membrane of eukaryotic organisms. Role of *trans*-Δ^3-hexadecenoic acid-containing phosphatidylglycerol. *Trends Photochem Photobiol* **2:** 13–32

Tronrud DE (1997) The TNT refinement package. *Methods Enzymol* **277:** 306–319

Vagin A, Teplyakov A (1997) MOLREP: an automated program for molecular replacement. *J Appl Crystallogr* **30:** 1022–1025

van Amerongen H, Dekker JP (2003) Light-harvesting in photosystem II. In *Light-Harvesting Antennas in Photosynthesis*, Green BR, Parson WW (eds) pp 219–251. Kluwer Academic Publishers, Dordrecht

Wentworth M, Ruban AV, Horton P (2001) Kinetic analysis of nonphotochemical quenching of chlorophyll fluorescence. 2. Isolated light-harvesting complexes. *Biochemistry* **40:** 9902–9908

Yang C, Kosemund K, Cornet C, Paulsen H (1999) Exchange of Pigment-binding amino acids in light-harvesting chlorophyll *a/b* protein. *Biochemistry* **38:** 16205–16213

